MEINSBERG KSI

FORSCHUNG & ENTWICKLUNG Chemische Sensoren
Elektrochemische Messtechnik
Biosystemtechnik
Analysenmesstechnik

Kurt-Schwabe-Institut für Mess- und Sensortechnik e.V. Meinsberg, Kurt-Schwabe-Straße 4, 04736 Waldheim

Scientific Report

subject: **Algorithm evaluation for e(CO_2)-tracking (AEFECT)**

investigation period:	30th September – 29th November 2019
date of report:	20th December 2019
experimenters:	A. Vogel, Dr. J. Zosel
written by:	Dr. Jens Zosel
Institute:	Kurt-Schwabe-Institut für Mess- und Sensortechnik e.V. Meinsberg (KSI), Germany
Address:	Kurt-Schwabe-Straße 4, D-04736 Waldheim
URL:	https://www.ksi-meinsberg.de/
Telephone:	+49 34327 608 102

Signatures:

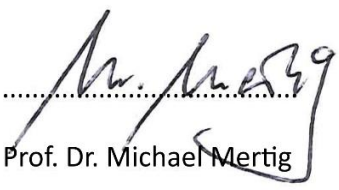

Prof. Dr. Michael Mertig	Dr. Jens Zosel	Annett Vogel
Head of KSI	Principal scientist	Experimenter

Abstract

Metal oxide gas sensors (MOX-GS) of the type ZMOD4410 (Renesas Electronic Corporation), SGP30 (Sensirion AG), and CCS811 (AMS AG) were characterized in different indoor air environments of KSI. The monitoring of these sensors was supplemented by parallel measurements with four different non-dispersive infrared (NDIR)-CO_2-sensors: SCD3x (Sensirion AG), K30 (Senseair), CM1106 (Cubic Sensor and Instrument Co., Ltd.), and HOBO CO_2 Logger MX1102 (Onset Computer Corporation). Four multi-sensor systems (MSS) equally equipped with the four sensors were operated simultaneously in different indoor environments (offices, meeting rooms, and laboratory) over two months and were calibrated at the start, middle, and end of the measurement campaign.

The signals of the investigated MOX-GS were used by algorithms developed by the sensor manufacturers to calculate real-time e(CO_2) values, which were correlated for every investigated sensor with the mean value of the IR-CO_2-sensors. That correlation was quantified by a factor between e(CO_2) and mean IR-CO_2 values and its standard deviation during a measurement. The correlations prove that the calculated e(CO_2) values exhibit temporal courses similar to those of the IR-CO_2-sensors. Summarizing one of the main findings of the campaign, it could be stated that this standard deviation becomes smaller with increasing number of people in the room. Furthermore, the ZMOD4410 with its specific algorithm delivers the smallest factor variations in the investigated range of circumstances, thus providing e(CO_2) values with the closest correlation to the real CO_2 concentration. The results clearly demonstrate that systems can be controlled for indoor air conditioning (HVAC) with the guidance of e(CO_2) values calculated in real-time from MOX-sensor signals.

Furthermore, measurements with more than five attendees in non-ventilated meeting rooms indicate that the exhaled CO_2 is distributed in the room's atmosphere quickly enough to estimate the number of attendees from the room volume and the CO_2 increase. This temporal gradient of the CO_2 concentration allows an occupancy estimation for improved ventilation and building automation.

Table of contents

1. Introduction

1.1 KSI

The Kurt-Schwabe-Institut für Mess- und Sensortechnik (KSI) is a governmental supported non-profit research institution, developing new sensor techniques in the following areas:

- Solid electrolyte gas sensors (electrode and electrolyte materials, detection methods, sensor design, and manufacturing technologies)
- Biological and physical sensors (DNA and protein chips, single molecule detection, measurement with complete cells, impedimetric, and optical sensors)
- Electrochemical sensors (miniaturized thick film sensors, ion selective electrodes, and electrochemical detection methods)

The KSI has a broad variety of state-of-the-art tools, technologies, and equipment for synthesis, manufacturing, and characterization of materials, thin and thick films, biological structures, and sensors. Some examples are devices to measure specific surface (BET), for material and layer characterization (XRD, SEM, EDX, XPS, µRFA, DTA/TG) and printing technologies (screen-printing and pulsed laser deposition).

KSI's equipment for gas sensor characterization comprises setups for providing high accuracy gas mixtures, gas analysis by GC/MS, MS, FTIR, and humidity measurement, as well as a special oxygen titration setup for material testing in gases with defined oxygen partial pressure. Methods to quantify gas sensors in a broad range of ambient pressures and temperatures are also available.

Intensive research studies on Carbon Dioxide (CO_2) have been completed in the last years and are summarized in the scientific book *Carbon Dioxide Sensing* [1]

1.2 Aims of the project

After different investigations of sensitivity, selectivity, long-term stability, cross sensitivities, and aging of different metal oxide gas sensor (MOX-GS), as well as their use for Indoor Air Quality (IAQ) characterization [2, 3, 4] carried out for Renesas Electronic Corporation, now a further extensive investigation was carried out on MOX-GS of three different vendors to estimate their usability for indoor air condition control. The main goal of this study was the correlation between e(CO_2) values calculated by supplier-developed algorithms with the values taken from four different non-dispersive infrared (NDIR) CO_2-sensors. This correlation was taken to answer the question: if the calculated e(CO_2) value can be used as an input-signal for controlling devices for air conditioning with a reliability comparable to that NDIR-CO_2-sensors would provide in this application.

2. Experimental

2.1 Experimental procedure

The following MOX-GS were investigated in this study:

- 12 ZMOD4410 modules (producer: Renesas Electronics America Inc., San Jose, USA)
- 4 SGP30 evaluation kits (producer: Sensirion AG, Staefa, Switzerland)
- 4 CCS811 evaluation kits (producer: AMS AG, Premstaetten, Austria)

Their signals and calculated eCO_2 values were correlated with temporal mean CO_2 concentration values, calculated from the signals of the following NDIR-CO_2-sensors (abbreviated as IR-CO_2-GS in the following text):

- 4 SCD3x pieces (producer: Sensirion AG, Staefa, Switzerland)
- 4 Senseair pieces K30 (producer: Senseair AB, Delsbo, Sweden)
- 4 CM1106 pieces (Cubic Sensor and Instrument Co., Ltd., Wuhan, China)

Additionally, four pieces of Onset HOBO CO_2 Logger MX1102 (Onset Computer Corporation, Bourne, MA, USA) were tested in parallel. Compared to the MOX-GS, the IR-CO_2-GS are significantly more expensive and have much larger dimensions. During the campaign, it was decided to exclude the signals of the MX1102 IR-CO_2-GS from the above-mentioned mean CO_2-concentration value calculation because their signals exhibit elevated noise and are not suitable for a comparison.

At KSI, the MOX-GS were positioned on plates to equip each of the four multi-sensor systems (MSS) with three ZMOD4410 pieces, one SGP30, and one CCS811. Each plate was placed in a transparent prismatic plastic box, which was topside opened during the measurement and closed during the calibration (see Fig. 4). The IR-CO_2-GS of each system were also positioned on different plates, which were held in larger prismatic boxes. The lids of these boxes were equipped with gas distribution tubes for directing single gas jets on every sensor. All sensors were operated in parallel at one single gas line. All sensor signals were collected and processed with communication boards and software packages supplied by the sensor producers. The software packages were installed on computers with Microsoft Windows 7 and 10 operating systems.

All sensors were calibrated three times during the measuring campaign, which covers two months in total. The MOX-GS were calibrated with ethanol containing mixtures in synthetic air, while different CO_2 concentrations also in synthetic air were applied for the IR-CO_2-sensors. All gas mixtures for calibration were established with mass flow controllers from Brooks Instruments, which were calibrated before investigation with a flow rate calibrator DryCal 800. For the calibration of the MOX-GS, the diluting gas synthetic air was constantly humidified by a device for precise dew point control, which is described in more detail in [2]. The outflow of the boxes was held at atmospheric pressure during calibration. The ethanol gas mixture was prepared in a commercial pressure cylinder with an injection unit developed by KSI. Before each calibration, the ethanol and CO_2 concentration steps were monitored with a downstream mass spectrometer and FTIR-spectrometer, respectively.

The experimental parameters of all experiments are described in section 2.3.

2.2 Experimental setup

The experimental setup for calibration is given schematically in Fig. 1 and illustrated in Fig. 2. The configuration for indoor measurements in offices and meeting rooms is schematically outlined in Fig. 3 and provided in Fig. 4 as a photograph together with the arrangement of the sensors in the measuring cells.

All commercial devices used in the setup are specified in Table 1. The ID numbers of the tested sensors are provided in Table 2. The following abbreviations and declarations are used in Fig. 1:

MFC Mass flow controller
sccm Standard cubic centimeter per minute (equals ml/min)
EtOH Ethanol
syn. synthetic

Fig. 1: Schematic drawing of the calibration setup

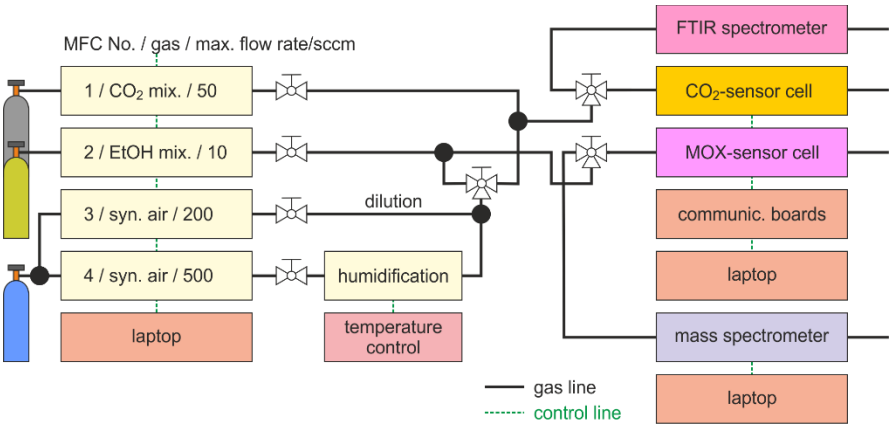

Fig. 2: Image of the calibration setup

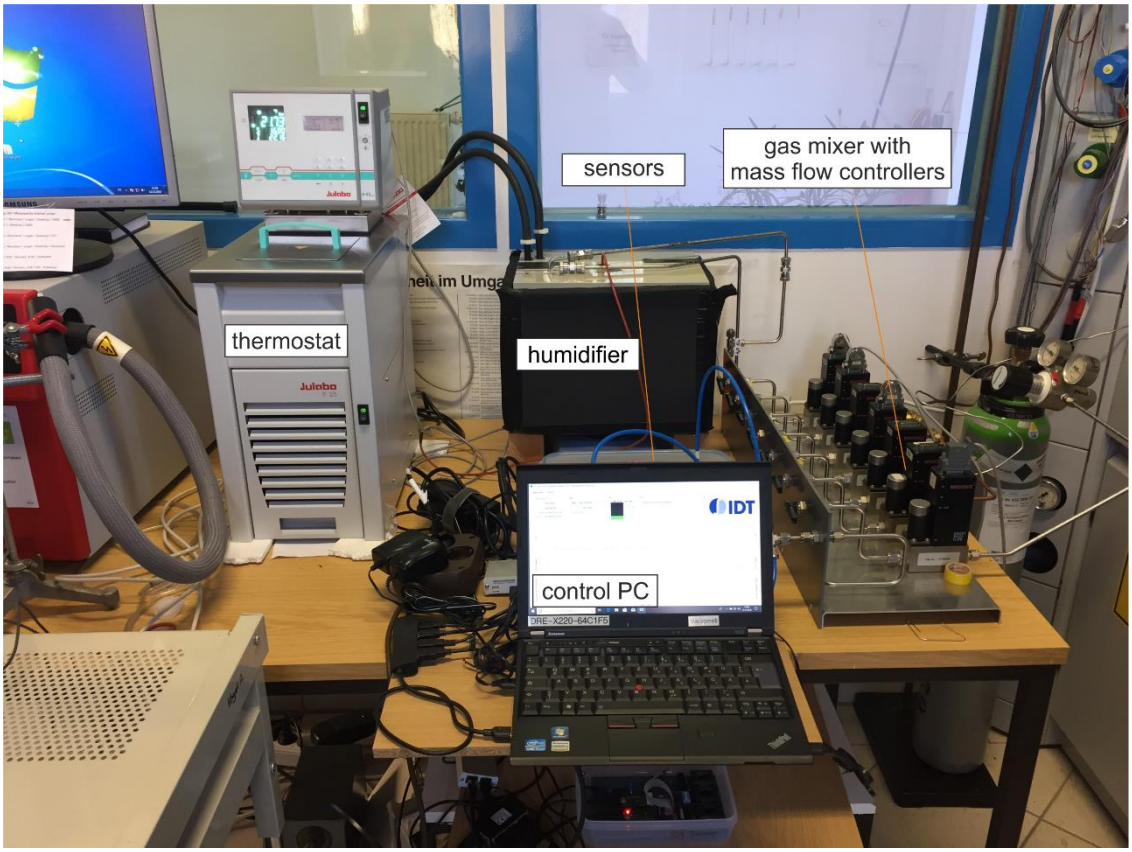

The humidifier for the synthetic air is a purpose-built arrangement of six horizontally positioned glass tubes that is described in detail earlier [3]. The home-build setup for preparation of the ethanol-mixture and its usage is described in detail in [4].

Table 1: Specifications of the devices used in the experimental setup

No.	Device	Type	Supplier	Most Relevant Technical Information
1	Thermo-/kryostat with external temperature sensor	F30-MH	Julabo Labortechnik GmbH, Seelbach, Germany	resolution: ± 0.01°C error: ± 0.02°C
2	Humidifier (home-build)		KSI	flow rate: 0 ... 1000 sccm H_2O saturation: > 99.99% dew point: 0.5 ... 20°C
3	Mass flow controllers (MFC)	5850S	Brooks Instrument, Hatfield, USA	flow accuracy ± 0.7% of rate and ± 0.2% full scale
4	Sensor cells (purpose-build)		KSI	polypropylen, inner measures (mm): 200 x 130 x 45 (MOX-GS) 260 x 200 x 80 (IR-CO_2-GS)
5	Flow rate meter for MFC calibration	DryCal 800	Mesa Laboratories, Inc. Butler, USA	range: 0.5 – 500 sccm, error: ± 0.15% of reading
6	Mass spectrometer	ThermoStar GSD320	Pfeiffer Vakuum GmbH, Germany	SEM and Faraday-detectors with HS ion source, limit of detection $1 \cdot 10^{-14}$ mbar
7	Pressure sensor at mixing cylinder	LPC-S-0010-0-ABS	DRUCK & TEMPERATUR Leitenberger GmbH, Germany	0 … 10 bar absolute error: ± 0.1% full scale
8	FTIR-Spectrometer	Nicolet 8700	Thermofisher, USA	Gas absorption cell with absorption path length = 20 cm

Fig. 3: Schematic drawing of measuring system

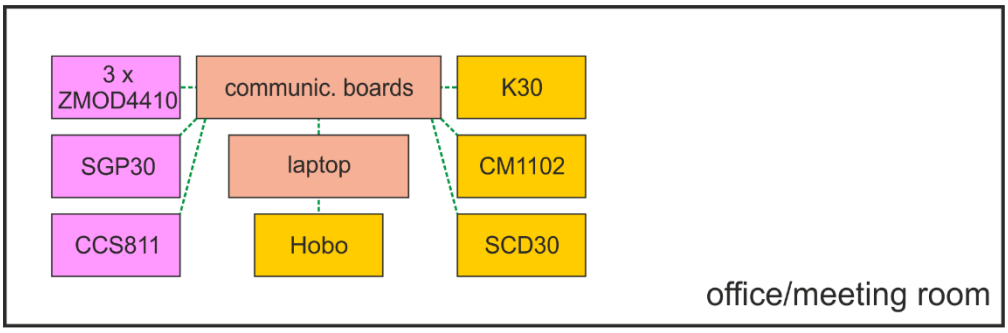

Fig. 4: Image of one of the multi-sensor systems (MSS)

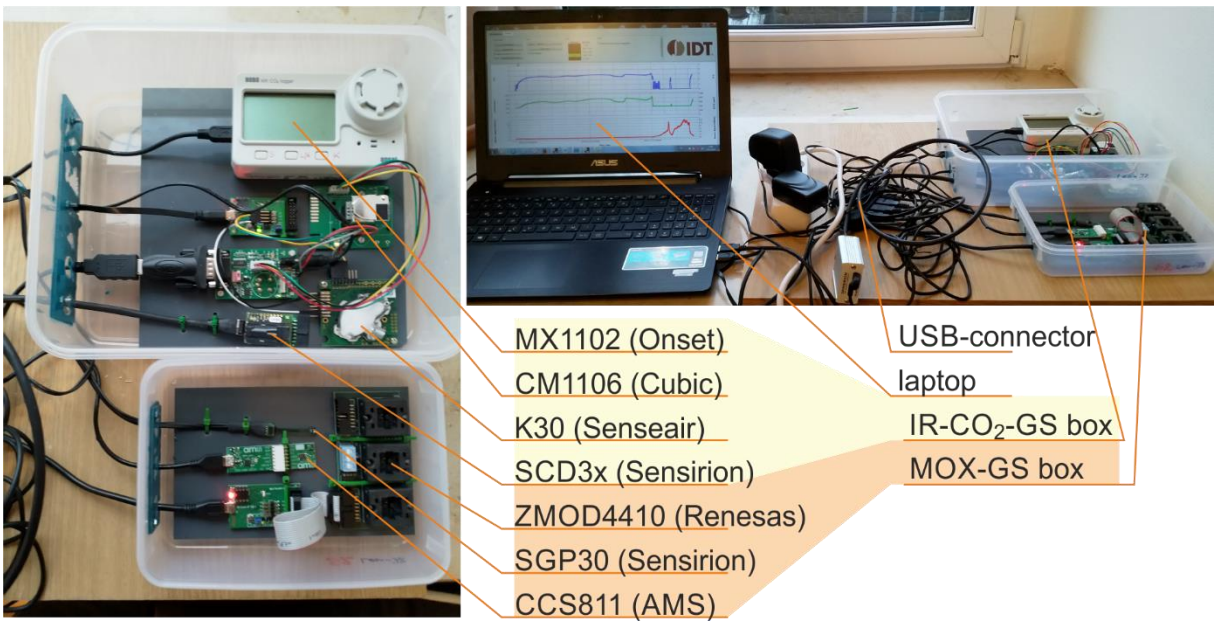

Table 2: Identification numbers of the tested sensors in the experiments

System No.	Sensor ID	Sensor Type	Producer
MSS 1	x0000464045C24EBB	MOX-GS/ZMOD4410	Renesas
	x0000464045C23FBB		
	x0000464045C25DBB		
	8478948	MOX-GS/SGP30	Sensirion
	389012-387300-50664863	IR-CO_2-GS/SCD3x	
	005A558C	MOX-GS/CCS811	AMS
	031C796C	IR-CO_2-GS /K30	Senseair
	0242581205110330	IR-CO_2-GS /CM1106	Cubic
	20530713	IR-CO_2-GS /HOBO MX1102	Onset
MSS 2	x0000464045C25CBA	MOX-GS/ZMOD4410	Renesas
	x0000464045C25EBF		
	x0000464045C26ABA		
	8498666	MOX-GS/SGP30	Sensirion
	398213-396791-50668093	IR-CO_2-GS /SCD3x	
	005A44CE	MOX-GS/CCS811	AMS
	031C797C	IR-CO_2-GS /K30	Senseair
	0242581107710151	IR-CO_2-GS /CM1106	Cubic
	20121753	IR-CO_2-GS /HOBO MX1102	Onset
MSS 3	x0000464045C24DBB	MOX-GS/ZMOD4410	Renesas
	x0000464045C25BBA		
	x0000464045C26ABB		
	8497303	MOX-GS/SGP30	Sensirion
	395315-396980-50663906	IR-CO_2-GS /SCD3x	
	005A47EB	MOX-GS/CCS811	AMS
	031C7975	IR-CO_2-GS /K30	Senseair
	0242581107710268	IR-CO_2-GS /CM1106	Cubic
	10974747	IR-CO_2-GS /HOBO MX1102	Onset
MSS 4	x0000464045C24DCB	MOX-GS/ZMOD4410	Renesas
	x0000464045C25BCB		
	x0000464045C24ACA		
	8479532	MOX-GS/SGP30	Sensirion
	367764-369223-50667534	IR-CO_2-GS /SCD3x	
	005A5B2E	MOX-GS/CCS811	AMS
	031C796B	IR-CO_2-GS /K30	Senseair
	0242581107710185	IR-CO_2-GS /CM1106	Cubic
	20530712	IR-CO_2-GS /HOBO MX1102	Onset

2.3 Experimental conditions

2.3.1 Calibration of MOX-GS

The calibration of the MOX-GS was carried out at room temperature in the smaller purpose-build PP-box given in Fig. 4. After flushing the box with humidified synthetic air for 3 hours, humidity controlled gas mixtures of synthetic air and ethanol were introduced into the box at c(EtOH) = 0; 30; 10; 6; 3; 1; 0.3; 0 vol.-ppm and 30 % r.H. for 30 minutes each (one calibration at start, middle, and end of the measuring campaign). The total volume flow was adjusted at constant 400 ml/min.

2.3.2 Calibration of IR-CO_2-GS

The calibration of the IR-CO_2-GS was carried out at room temperature in the larger purpose-build PP-box given in Fig. 4. Dry gas mixtures of synthetic air and CO_2 were introduced into the box at c(CO_2) = 0; 3000; 2500; 2000; 1500; 1000; 500; 0 vol.-ppm for 1 hour each (one calibration at start, middle, and end of the measuring campaign). The total volume flow was adjusted at 500 ml/min. Before the first calibration, a manual pre-calibration in outdoor air was carried out with every MX1102 IR-CO_2-GS according to the operating manual, which sets the value to 400 vol.-ppm.

This manual one-point pre-calibration was not repeated in the two-month measuring campaign. The other IR-CO_2-GS could not be pre-calibrated and were used in their state of delivery. Eventually occurring cross sensitivity of the IR-CO_2-GS to water vapor was tested in CO_2-containing mixtures with 0 and 30 % relative humidity at 25 °C.

2.3.3 Measurement in indoor environments

The four MSS were positioned in two offices and two meeting rooms. MSS 4 was positioned event-dependent in meeting rooms of different sizes and populations. The measurement durations of every system ranged from 3 hours for a short meeting up to maximum of 67 hours during the weekends. The data were collected, processed and then summarized in Tables A2 to A5, Fig. A1 and A2 (in the addendum beginning at page 22) as well as in Fig. 15 in the next section.

3. Results

3.1 Calibration

3.1.1 MOX-GS

One example of the calculated TVOC signals (TVOC = Total Volatile Organic Compounds) is provided for each type of the investigated MOX-GS as numbered in Table 2 in Fig. 5. Only the ZMOD4410 covers the complete investigated concentration range, while CCS811 and SGP30 MOX-GS end up in a saturation limit at the higher ethanol concentrations. Interestingly, the tendency of TVOC to decrease with increasing number of calibration found for ZMOD4410 and CCS811 is not valid for SGP30. Here, the values of the second calibration are higher than those of the first and third calibration.

In Fig. 6 the calculated e(CO_2) values of the sensors given in Fig. 5 are shown. The algorithms of the vendors for determining these values are based on the hypothesis that beside carbon dioxide a fixed mean concentration of VOC is breathed out by humans. Therefore, it is expected that the application of artificial mixtures of ethanol and water vapor in synthetic air without any carbon dioxide to the MOX-GS will not result in meaningful eCO_2 values. Otherwise, the resulting curves should provide deeper insight into the transformation procedure of the algorithms. The curves in Fig. 6 indicate that the algorithms used by the different vendors show significant differences.

Fig. 5: TVOC values of MOX-GS (MSS 1) during ethanol calibrations; left: ZMOD 4410 No. x0000464045C23FBB, middle: CCS811 No. 005A558C, right: SGP30 No. 8478948

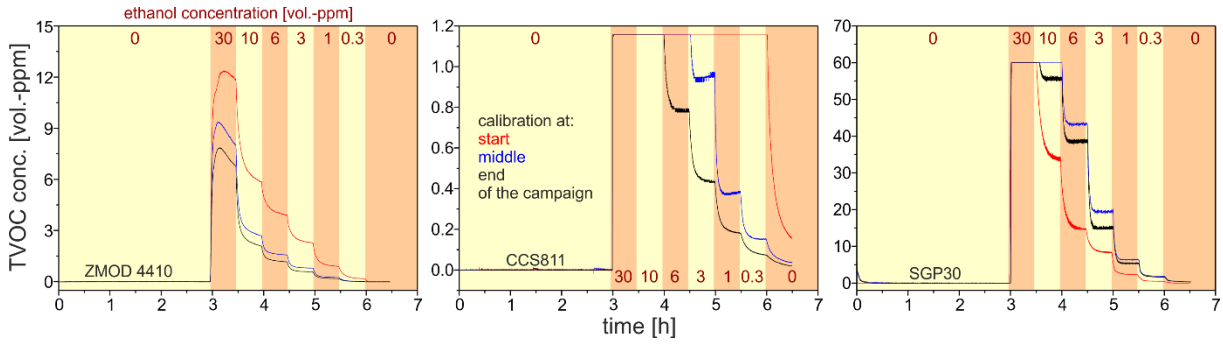

Fig. 6: e(CO_2) values of MOX-GS (MSS 1) during ethanol calibrations; left: ZMOD 4410 No. x0000464045C23FBB, middle: CCS811 No. 005A558C, right: SGP30 No. 8478948

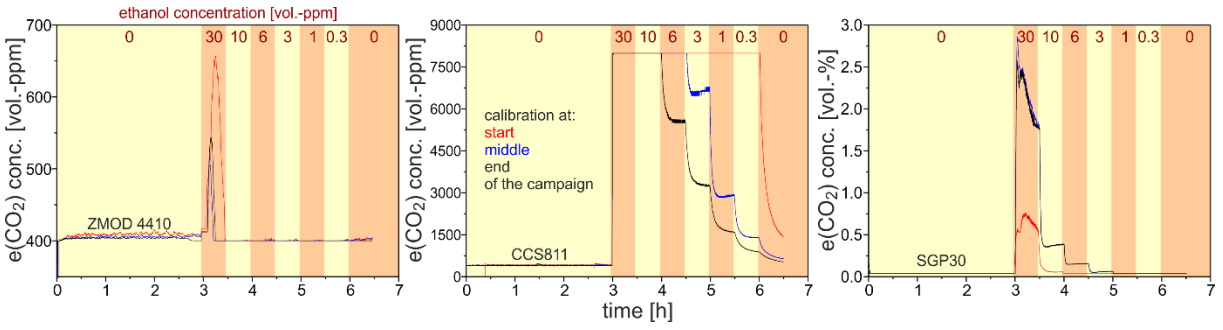

3.1.2 IR-CO_2-GS

The calibrations of all IR-CO_2-GS with dry CO_2-N_2 mixtures result in rapid responses to the changes of the CO_2 concentration and a nearly horizontal plateau as shown in Fig. 7 for MSS 1. The sensors K30 and MX1102 exhibit comparably low deviations between the calibrations at all concentrations, indicating a high reproducibility at the adjusted calibration conditions. In contrast to these sensors, the CM1106 exhibits large differences between calibration No. 2 and calibrations 1 & 3. It could be that a dust particle or other temporary contamination influenced calibration No. 2. The SCD3x results in a significant difference between calibration No. 1 and 2 & 3, indicating a more persistent contamination.

The MX1102 exhibits much larger noise in the signal than the other three IR-CO_2-GS. Therefore, this signal was excluded from the mean value calculation mentioned in section 3.2.1.

For comparison of all sensors and for calculating the real CO_2 concentrations from the signals of the uncorrected sensors, a linear regression between the sensor signals S(CO_2) and the CO_2 concentrations c(CO_2) provided during calibration was calculated, resulting in equations of the form of equation (1):

$$c(CO_2) = slope \cdot S(CO_2) + intercept_Y \quad (1)$$

Fig. 7: Signals of IR-CO_2-GS (MSS 1) during CO_2 calibrations; upper left: SCD3x No. 389012-387300-50664863, upper right: K30 No. 031C796C, lower left: CM1106 No. 0242581205110330, lower right: MX1102 No. 20530713

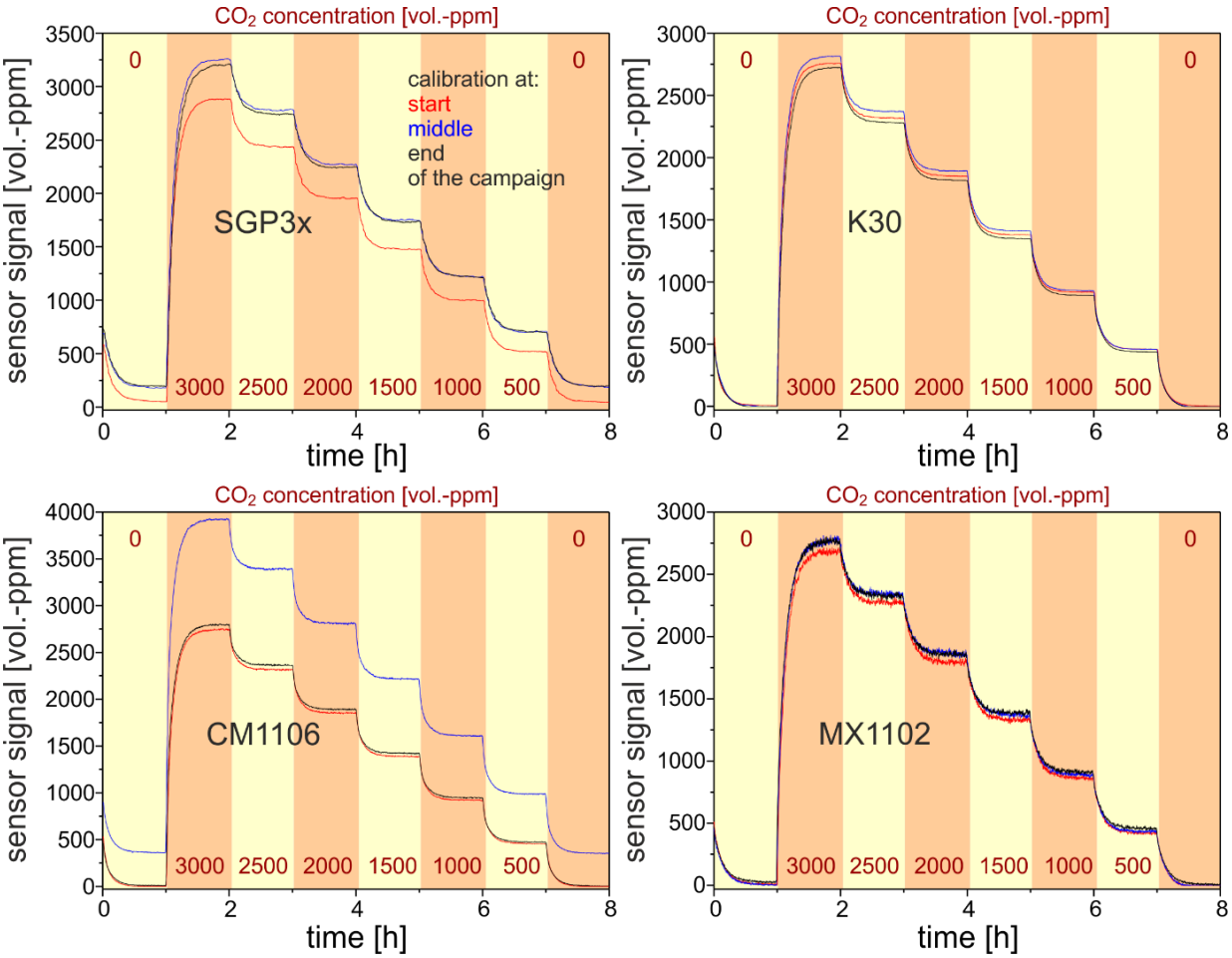

As the curves of K30 and MX1102 in Fig. 7 indicate, the signal at zero CO_2-content is set to zero, which is signaled if the concentration falls below a threshold concentration. In that case, the signal at zero CO_2 concentration was excluded from linear regression, which is calculated for those sensors only for the applied CO_2 concentrations from 500 to 3000 vol.-ppm. An example of regressions is given in Fig. 8 for the third calibration of MSS 1. All values for slope, offset, and regression coefficient are specified in Table A1 in the annex. Each investigated IR-CO_2-GS provides appropriate linearity.

Since the tendencies of signal in- or decrease between the consecutive calibrations differ between the sensors, it is assumed that all deviations result mainly from the sensors themselves and are not influenced by systematic inaccuracies of the provided gas concentrations. The minimum variance of the regression values was found for the four K30 IR-CO_2-GS, as the bars in Fig. 9 indicate for the example of MSS 1. The deviations of uncorrected signals of the four different IR-CO_2-GS shown here at the applied CO_2 concentration 1000 vol.-ppm indicate that it is advisable to calibrate such sensors regularly, if a measuring error below 100 vol.-ppm is required.

Fig. 8: Calibration functions of IR-CO_2-GS (MSS 1) during calibration No. 3; c(CO_2) = concentration provided in the calibration gas mixture, S(CO_2) = sensor signal at the end of the concentration step

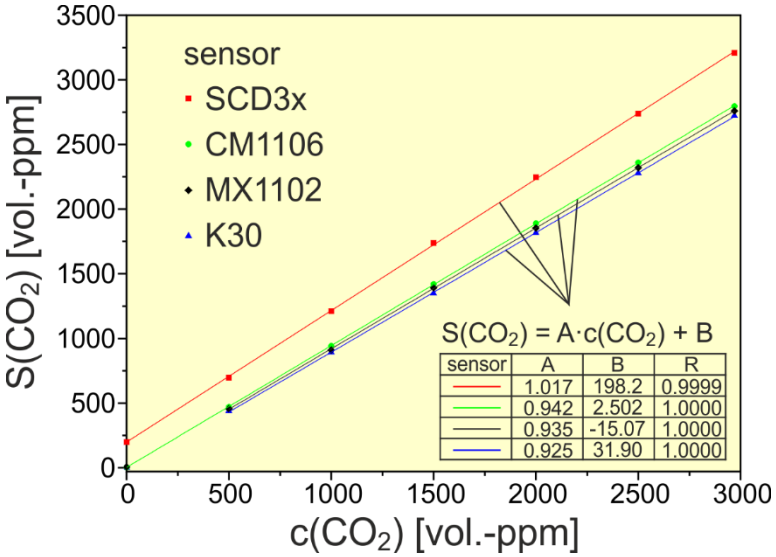

Fig. 9: Mean absolute deviation between S(CO_2) and c(CO_2) and its standard deviation during the three calibrations of MSS 1 at c(CO_2) = 1000 vol.-ppm

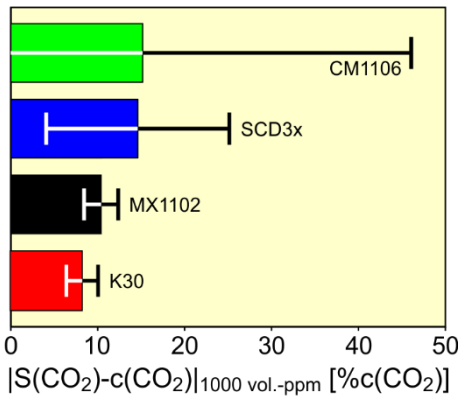

In Fig. 10, example curves of the IR-CO_2-GS in CO_2-containing mixtures with different relative humidity are provided. They indicate that the cross-sensitivity to water vapor can be neglected. Therefore, the calibration with the selected dry mixtures is also valid for gases with higher humidity.

Fig. 10: Testing of IR-CO_2-GS (MSS 4) in CO_2-containing mixtures with different relative humidity

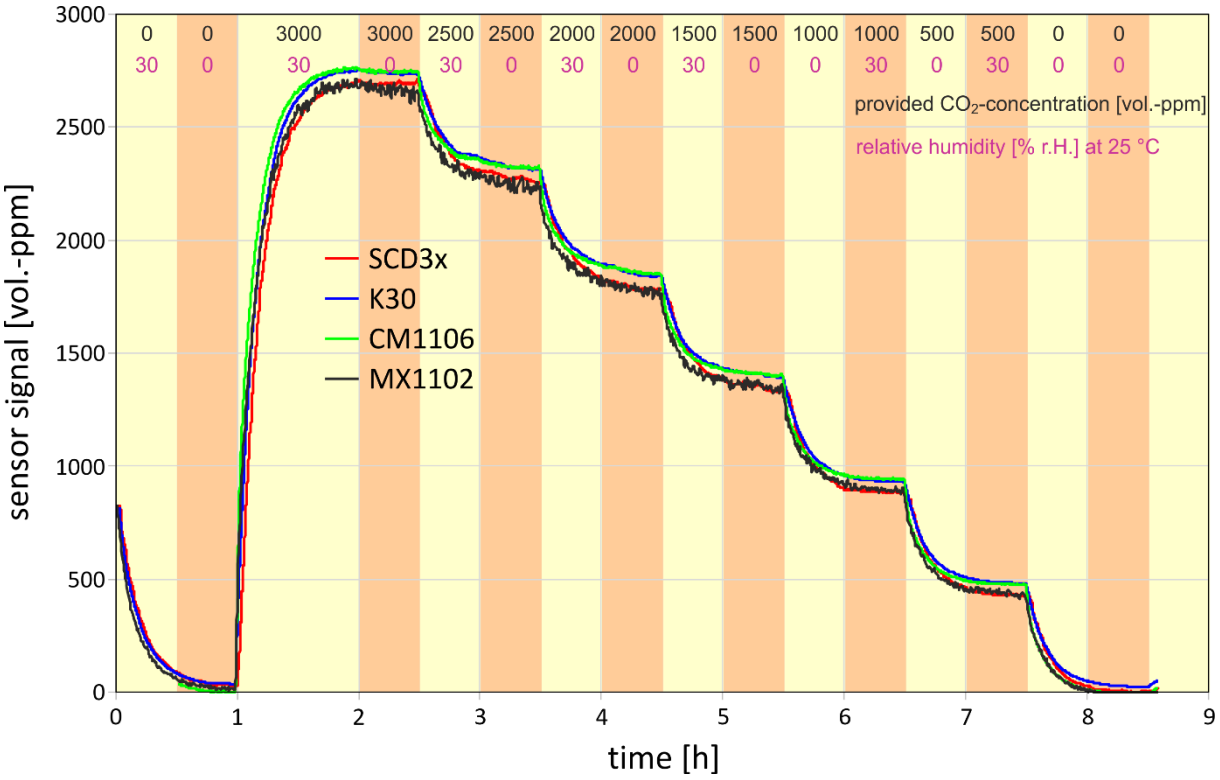

3.2 Indoor air measurements in offices and meeting/conference rooms

3.2.1 Determination of the actual CO_2 concentration

Since each of the four MSS was equipped with four different IR-CO_2-GS, it is self-evident to calculate a mean CO_2 value $c(CO_2)_m$ for every timestamp. Comparably small differences between the response times as well as the signal-to-noise-ratios (SNR) of the different sensors is a pre-condition for this calculation. Taking the results of the calibrations (given in section 3.1) into account, it was agreed between the contractors that the signals of the SCD3x, K30, and CM1106 were used to calculate $c(CO_2)_m$. The signal of the MX1102 was excluded from this calculation due to its elevated signal noise. In Fig. 11A courses of the signals of the different IR-CO_2-GS of system 4 are illustrated, which were taken in a comparably small unventilated meeting room with the volume V = 90 m^3 populated with up to 20 people. This result in high CO_2 increases per time unit (temporal gradients). The CO_2 concentrations calculated from the calibration equations in Table A1 are given in Fig. 11B. They prove that these calculations result in comparable CO_2 values at all slopes.

A person, checking the measuring system, caused the peak in Fig. 11B at 4.4 h. This maximum temporal gradient is shown in Fig. 11C with larger resolution. The CO_2 increase (mean value) caused by breathing directly onto the sensors amounts to 1550 ppm/min. It can be seen that the $c(CO_2)_m$ value represents the courses of the three sensors in an appropriate manner even at such a steep concentration increase. This orienting measurement was conducted on September 25th, 2019 before the start of the campaign and is not included in the annex tables A2 toA5. A picture of the meeting room is shown in Fig. 12.

Fig. 11: Measurement with IR-CO_2-GS (MSS 4) in a nonventilated meeting room with V = 90 m^3 with different numbers of persons (blue values) and different window configurations (green arrows). Outside the green arrows windows and door were closed. A: sensor signals; B: signals corrected by equation 1 and values in table A1, C: magnification of the labelled time span in B

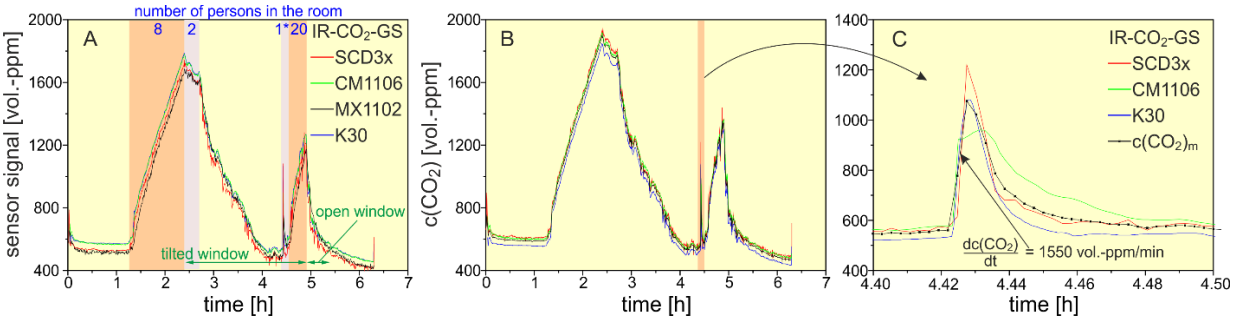

3.2.2 Other aspects of sensor performance

Two phenomena of the sensor performance have to be mentioned for its comprehensive assessment. One of it concerns the K30 IR-CO_2-GS showing between one and maximal four abnormal signal spikes during a 24-hour measurement. All spikes are represented by a single value ranging more than 100 vol.-ppm above the preceding and following values. It is suspected that these spikes are due to EMC interferences but it was not possible to correlate them with particular events in the measuring environment. These spikes were erased from the measurement by replacing them with the mean value of the preceding and the following value.

Fig. 12: Picture of the meeting room used for the measurement presented in Fig. 11

All K30 and one of the CM1106 IR-CO_2-GS exhibited the second phenomenon shown in Fig. 13. It is indicated by distinct upward and downward leaps in the signal (from one value to the next), which are caused probably by particles in the measuring gas settling in the optical path between the IR emitter and detector. The largest leaps were found in the signal of CM1106 integrated in MSS 1. They occurred at October 17th, 2017 at 00:06am (575 vol.-ppm upward in the raw signal) and at November 16th, 2019 3:09pm (503 vol.-ppm downward in the raw signal), when no one was in the laboratory. The leaps of the K30 sensors range below 60 vol.-ppm in the raw signal. This phenomenon was neutralized by adaptation of the $intercept_Y$ in case of the K30 sensors, and by switching to the slope and $intercept_Y$ of the following calibration in case of the CM1106 sensor.

Fig. 13: Signal leaps of CM1106 IR-CO_2-GS (MSS 1)

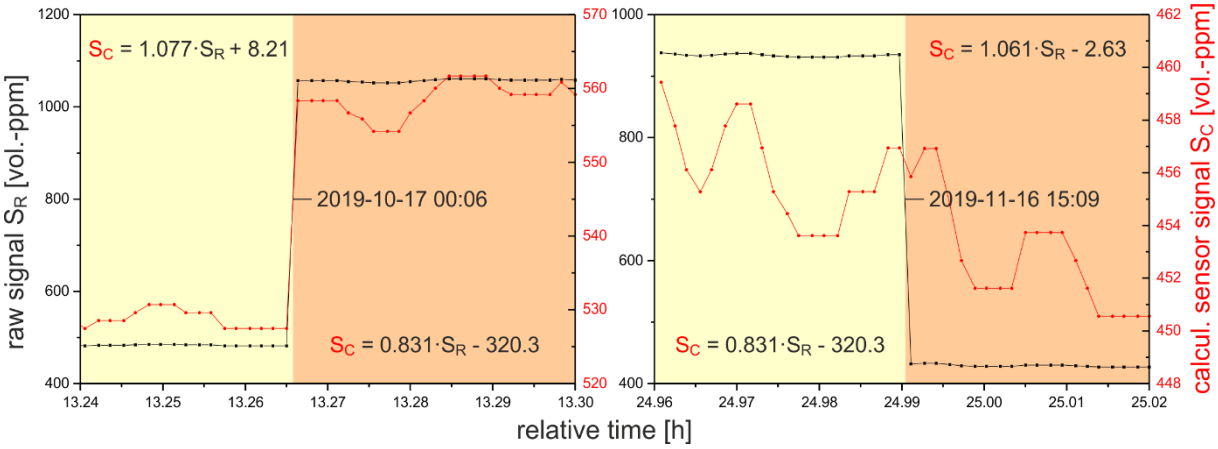

3.2.3 Correlation between mean CO_2 concentration and e(CO_2) values

In Fig. 14 the same experiment as in Fig. 11 is taken to compare the calculated e(CO_2) values with the mean values of the IR-CO_2-GS (black curve in Fig. 11B). The first view on these curves confirms that the e(CO_2) values of all three investigated sensors develop qualitatively in the same manner as the mean values of the IR-CO_2-GS. Therefore, the basic hypothesis of a resilient correlation between CO_2 and VOC concentrations in indoor air is strongly supported by these curves. A second view reveals that none of the tested MOX-GS and algorithms detect those small peak-like changes of c(CO_2)$_m$ as the one enlarged in Fig. 11C.

Furthermore, the ability of the algorithms to follow decreasing c(CO_2) courses during ventilation or diffusion of CO_2 through leaks in windows, walls, and doors differs strongly between the vendors. While the SGP30 shows a slow signal decrease resulting in an overstepping of e(CO_2) above c(CO_2) between 600 and 1000 vol.-ppm, both the CCS811 and ZMOD4410 MOX-GS exhibit a rapid backtracking to the minimum value. In Fig. 14, only one of the three ZMOD4410 sensors is presented since the signals of the other two sensors do not differ significantly from its curve. This similarity between the three ZMOD4410 was found valid for each MSS and measurement.

The comparison of signals in the period with eight attendees in the room (t = 1.3…2.4 h) with that of 20 participants (t = 4.5 … 5 h) indicates that the difference between e(CO_2) and c(CO_2)$_m$ values becomes smaller with an increasing number of monitored people. This expectable result was valid during all measurements.

Fig. 14 displays also the values taken for the comparison of all indoor air measurements with the different systems. For that purpose, a factor f was calculated for each MOX-GS for every timestamp according to equation (2):

$$f(MOX-GS,t) = \frac{e(CO_2)(t)}{c(CO_2)_m(t)} \quad (2)$$

The mean value f_m of this factor and its relative standard deviation $SD(\%f_m)$ during every complete experiment were calculated for the ranges $c(CO_2)_m$ > 1000 vol.-ppm and $c(CO_2)_m \leq$ 1000 vol.-ppm respectively.

$$f_m = \frac{\sum_{i=1}^{n} f_i}{n} \quad (3)$$

$$SD(\%f_m) = \frac{\sqrt{\frac{\sum_{i=1}^{n}(f_i - fm)^2}{n}}}{f_m} \cdot 100 \quad (4)$$

These values are given in Tables A2 to A5 for MSS 1 to 4. The picture provided by them is relatively complex and initiates further thinking on possible correlations and algorithm optimization. In Fig. 15 the maximum, minimum, and mean values of f_m and $SD(\%f_m)$ are provided for the complete measurement campaign of each MSS.

Fig. 14: Comparison of the e(CO_2) values calculated from the signals of the MOX-GS (MSS 4) in the measurement of Fig. 11 with the mean CO_2 value (c(CO_2)$_m$)

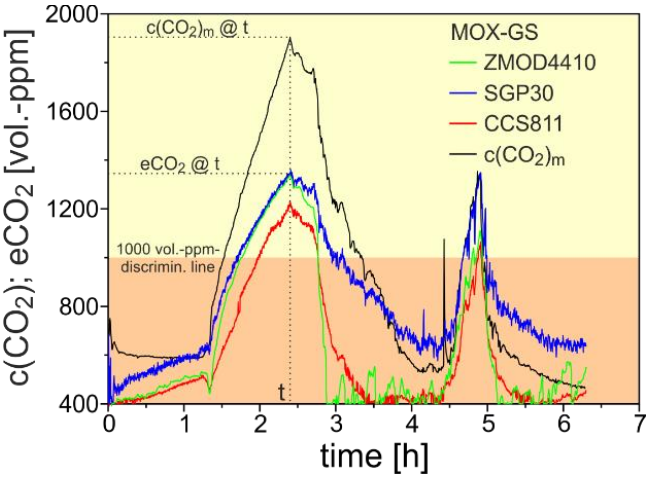

The nearer the factor f_m ranges to 1 and the smaller the relative standard deviation $SD(\%f_m)$ results, the smaller is the difference between the e(CO_2) and the c(CO_2)m values. Since all sensors delivered very similar response curves during calibration, the large differences of f_m and $SD(\%f_m)$ between the individual MSS come with the measurement conditions in the different rooms. If the e(CO_2) value is intended to be used for the regulation of heating, ventilation, and air conditioning systems (HVAC) regulation, its correlation with the c(CO_2)$_m$ value above 1000 vol.-ppm is much more important than below 1000 vol.-ppm. This limit is known as the Pettenkofer value for maximum tolerable indoor air concentration of CO_2 [5] and recommended also by the German Federal Environmental Agency (UBA) [6]. The finding that in that region all three MOX-GS of the MSS 2-4 deliver f_m values (white lines in Fig. 15) very near to 1 and acceptably low *SD* values is very encouraging for this application. Another result pointing in this direction is indicated by the minimum values of fm. In the region above 1500 vol.-ppm f_m of ZMOD4410 ranges above 0.55 at all investigated conditions, if this threshold is exceeded for more than 5 min. This means that an HVAC controlled by an e(CO_2) value will always start latest at the double value of that threshold.

The results of MSS 1 above 1000 vol.-ppm should be excluded from interpretation here, since only two measurements of the campaign in this highly ventilated laboratory resulted in values in that region and only for a very short time (see table A2).

In both regions (above and below 1000 vol.-ppm) the ZMOD4410 sensors exhibit the lowest differences between the calculated e(CO_2) and measured c(CO_2)$_m$ values. This optimum predictability was found for each measuring system at all investigated measuring conditions.

Fig. 15: Ranges of fm and SD(%fm) for each sensor during the complete measurement campaign, left column: $c(CO_2)_m$ > 1000 vol.-ppm, right column: $c(CO_2)_m$ < 1000 vol.-ppm, the mean values are indicated with white horizontal lines

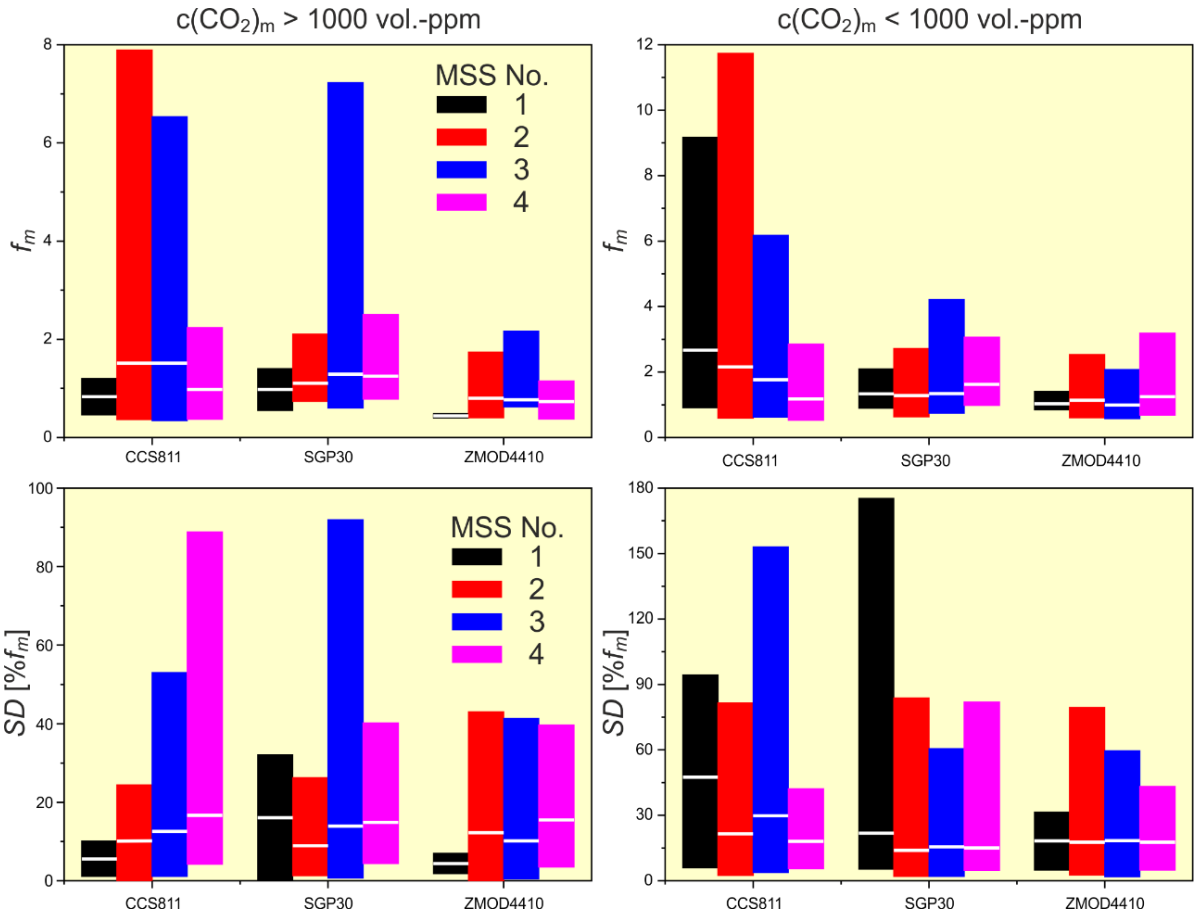

On the other hand, the comparison of f_m and *SD* between MSS 2&3 and MSS 4 reveals that the concept of $e(CO_2)$ calculation provides increasing precision with the increasing number of people in the room. MSS 4 was used in different meeting rooms with many times more than three residents, while MSS 2&3 were situated in offices with one or two residents most of the time. Accordingly, maximum f_m values were found for MSS 2&3 with CCS811 and SGP30 signals. Of course, f_m rises in a small room with one or two people much more than in larger rooms with more attendants if particular high VOC emissions come with these single persons (excessively used deodorant, special clothing, special breath gas composition, etc.). For more insight, the measurements No. 2 and 20 of MSS 2, No. 12 of MSS 3, and No. 48 of MSS 4, are provided as temporal courses of $e(CO_2)$ and $c(CO_2)_m$ values in the annex.

3.2.4 Estimation of people in a room from the CO_2 increase

The CO_2 and VOC emissions of humans are well investigated and published [7, 8, 9]. They depend on age, gender, and foremost on the state of physical and mental activity. Assuming moderate numbers of CO_2 emissions during presentations or meeting conversation, it could be estimated from the values given in [7] that one average attendee exhales between 14 and 18 liter CO_2 per hour. Assuming furthermore that the exhalation is distributed rapidly in a non-ventilated room with the volume V_R = 10 m^3, it can be calculated from these limits that the CO_2 increase coming from the exhaled gas of that average attendee amounts to 1400-1800 vol.-ppm/h. Consequently, the corresponding coefficient of CO_2 increase C_i in a non-ventilated room populated with one attendee amounts to:

$$C_{i,one\ attendee} = \frac{dc}{dt} V_R = 1.4 \ldots 1.8\ \frac{vol.-\%}{h} m^3 \quad (5)$$

During the campaign, several measurements with more than five attendees (N_a = number of attendees) in non-ventilated rooms with closed windows and doors were evaluated by extracting the CO_2 increase *dc/dt* from the temporal course of the $c(CO_2)_m$ value. This increase was taken to calculate the coefficient C_i according to equation (6).

$$C_i = \frac{\Delta c}{\Delta t} \frac{V_R}{N_a} \quad (6)$$

The values of C_i, given in Table 3, range in the region numeralised in equation (5). This result indicates the possibility to estimate the number of attendees in a non-ventilated room from the CO_2 increase and the room volume.

Table 3: Evaluation of measurements with MSS4 in two different non-ventilated rooms with more than five attendees, C_i was calculated with equation (6), measurements are described in Table A5

No.	Date of measurement	duration of CO_2 increase Δt [h]	N_a	V_R [m^3]	$c(CO_2)$-increase Δc [vol.-ppm]	$\Delta c/\Delta t$ [vol.-ppm/h]	C_i [vol.-%·m^3/h]
0	25.09.19	0.20	8	90	260	1300	1.46
9	16.10.19	0.35	28	339	455	1300	1.57
24	04.11.19	0.21	30	339	315	1500	1.56
34	18.11.19	0.60	10	90	1020	1700	1.53

3.3 Example for the signal course of IR spectrometer

As described in section 2.2, all IR-CO_2-GS calibrations were also monitored by a high-end IR spectrometer. A complete IR spectrum between 7800 and 350 cm-1 is measured with that device, enabling the precise monitoring of the complete CO_2 absorption peak. The background in CO_2 free air is subtracted from these spectra providing a much more precise and reliable CO_2 measurement with such expensive spectrometer than with the investigated low-cost IR-CO_2-GS, which measures the IR absorption only at selected wavelengths. As an example, the curve of a calibration measurement with the CO_2 concentrations mentioned in section 2.3.2 is illustrated in the left diagram of Fig. 16. The measurement was carried out at a flow rate of approximately 100 ml/min through the absorption cell in the IR-spectrometer. From this measurement, a calibration equation was determined by regression, which is valid for a measuring period of several months due to the excellent stability of the IR spectrometer. The corresponding signal function is provided as the blue curve in the left diagram in Fig. 16. In the right diagram of Fig. 16, curves of the last calibration in the campaign of the IR-CO_2-GS of MSS 1 are illustrated for direct comparison. It is clearly visible that precision, response time, and repeatability of the concentration signal of the extensively stabilized IR spectrometer are superior compared those of the signals of the IR-CO_2-GS.

The mass spectrometer was applied for the monitoring of the ethanol containing gas mixtures used for the characterization of MOX-GS in the laboratory. The distributed gas outlet of the sensor boxes described in section 2.2 disables a direct concentration measurement behind the box. Therefore, the mass spectrometer was positioned in the gas flow at the outlet of the mixing station (see. Fig. 1) alternatively to the sensor boxes. The performance of the mass spectrometer for monitoring the ethanol concentration in the calibration gas was already described in the ICSIS report (Fig. 22, p. 19). The results found here prove that the same precision and reliability was established during the calibrations of this campaign.

Fig. 16: Areas of the IR extinction peaks measured in the gas absorption cell of the Nicolet 8700 spectrometer by applying the CO_2 calibration gas mixtures, its calibration curve (left) and comparison with calibration curves of the IR-CO_2-GS of MSS 1 during last calibration in the campaign (right)

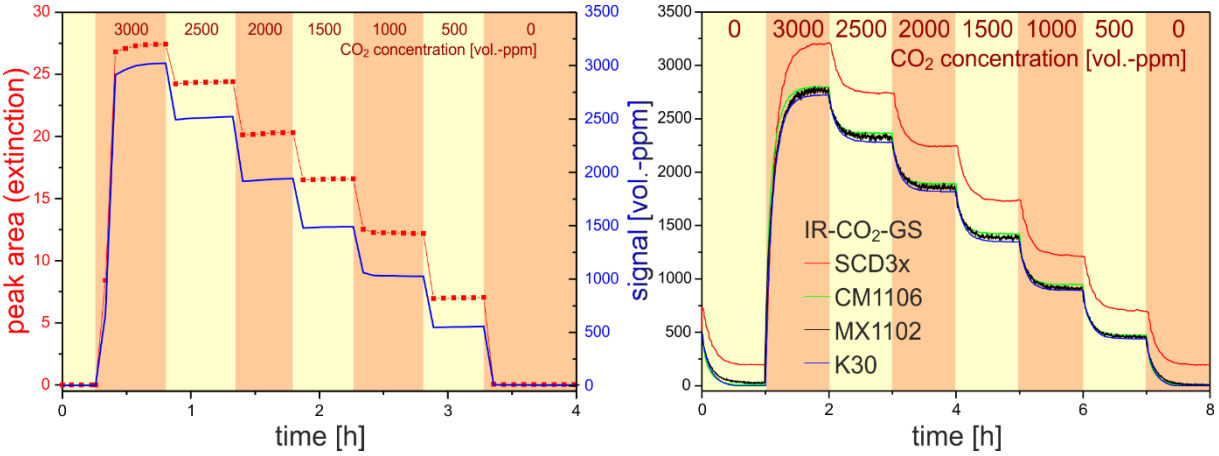

4. Conclusions

A measurement campaign of indoor air monitoring in different offices, meeting rooms, and one ventilated laboratory was conducted over two months. Four measuring systems were equally equipped with four non-dispersive infrared-CO_2-sensor (IR-CO_2-GS) and five metal oxide gas sensor (MOX-GS) from three different vendors. The IR-CO_2-GS were calibrated with CO_2 containing mixtures. It was found out by three different calibrations that these sensors, which are larger and more expensive than the investigated MOX-GS, show several sudden signal leaps and significant measuring errors of more than 10 %. Between the signals of the different sensors differences of more than 15 % were recorded. Checking the MOX-GS with ethanol containing mixtures proved that all MOX-GS from one vendor show similar calibration curves. Between the MOX-GS of different vendors, larger signal differences were found in the ethanol containing mixtures leading to different TVOC concentrations.

From the signals of three IR-CO_2-GS, a mean value $c(CO_2)_m$ was calculated for each available time stamp. This value was compared with the $e(CO_2)$ values calculated by different vendor-specific algorithms from the signals of the MOX-GS. This comparison was carried out in two regions with 1000 vol.-ppm as threshold. This limit was taken from literature in order to trigger an action such as a ventilation. The first region was $c(CO_2)_m < 1000$ vol.-ppm and the other one $c(CO_2)_m > 1000$ vol.-ppm. In both regions the values were compared by calculating the ratio $f = e(CO_2)/c(CO_2)_m$ for every timestamp. The nearer the mean value of f ranges to 1 and the smaller its standard deviation during a measurement, the closer is the correlation between $e(CO_2)$ and $c(CO_2)_m$ and the higher is the reliability of $e(CO_2)$ values as input parameters for HVAC. The comparison proves that it is possible to control air condition systems by the calculated $e(CO_2)$ values in rooms of different sizes and numbers of residents, if the threshold value for ventilation start can range in a band. For the investigated CCS811 MOX-GS this band has the highest width (i.e. largest deviation of $e(CO_2)$ values), while those for the SGP30 and ZMOD4410 MOX-GS are significantly smaller and therefore more precise. The minimum differences between the $e(CO_2)$ and $c(CO_2)_m$ values were found for the ZMOD4410 MOX-GS in both regions. As expected, the reliability of $e(CO_2)$ values increases with increasing number of attendees in the monitored room.

Furthermore, an occupancy estimation was possible based on CO_2 levels. Several measurements indicate that also in non-ventilated rooms the exhaled CO_2 is distributed in the room's atmosphere quickly enough to estimate the number of attendees from the room volume and the temporal gradient of the CO_2 concentration, which is measured with the used IR-CO_2-GS after start of a meeting.

To control modern energy-efficient HVAC systems a state-of-the-art sophisticated MOX-GS, such as the ZMOD4410, can be taken into account for air ventilation based on the carbon dioxide level.

5. References

[1] G. Gerlach, U. Guth, W. Oelßner: Carbon Dioxide Sensing; Fundamentals, Principles, and Applications, Wiley-VCH, Berlin, 2019, ISBN: 978-3-527-41182-5.

[2] J. Zosel, M. Mertig: Investigation of sensitivity, selectivity, long-term stability and cross sensitivities of micro-metal oxide gas sensors provided by the company Integrated Device Technology (IDT), Dresden, Germany. Confidential Scientific Report, p. 6, Meinsberg, 24th October 2017.

[3] J. Zosel, M. Mertig: Independent investigation of MOX gas sensors compliance with the UBA's IAQ study, Dresden, Germany. Confidential Scientific Report, p. 5, Meinsberg, 20th August 2018.

[4] J. Zosel, M. Mertig: Independent comparative study on IDT's and Sensirion MOX-gas sensors to characterize reproducibility; lifetime and reliability as well as humidity influence (ICSIS), Dresden, Germany. Confidential Scientific Report, Meinsberg, 20th December 2018.

[5] M. von Pettenkofer: Über den Luftwechsel in Wohngebäuden (About the air change in residential buildings), München: Cotta (in German) (1858).

[6] Umweltbundesamt, Gesundheitliche Bewertung von Kohlendioxid in der Innenraumluft, (Bundesgesundheitsblatt - Gesundheitsforschung - Gesundheitsschutz, 2008).

[7] S. Schaal, K. Kunsch, S. Kunsch: Der Mensch in Zahlen (A human in numbers), Springer Spektrum, Berlin, 2016, p. 109, DOI 10.1007/978-3-642-55399-8 (in German).

[8] R. Müller: Atmung, Stoffwechsel und Blutkreislauf (respiration, metabolism, and blood circuit), Prax. Naturwiss., Phys. Sch. 50 (8) (2001) 23–26 (in German).

[9] J.D. Fenske, S. E. Paulson: Human Breath Emissions of VOCs, J. Air Waste Manag. Assoc. 49 (5) (1999) 594-598.

Addendum

Table 1: Values of the three different calibrations of IR-CO_2-GS according to equation (1): slope, $intercept_Y$ and regression coefficient R, red: largest deviations, green smallest deviation.

Type	MSS No.	Calibration No.	slope	$intercept_Y$	R
SCD3x	1	1	1.046	-43.43	1.0000
		2	0.965	-181.66	1.0000
		3	0.983	-194.63	0.9999
	2	1	1.056	-22.44	0.9997
		2	1.034	-39.02	0.9998
		3	1.046	-36.23	0.9998
	3	1	1.049	-26.67	1.0000
		2	1.028	-26.90	0.9999
		3	1.067	-22.05	1.0000
	4	1	1.102	28.72	0.9999
		2	1.032	70.78	0.9999
		3	1.045	79.25	0.9998
K30 (sensors with minimum variance)	1	1	1.077	5.42	1.0000
		2	1.046	22.34	1.0000
		3	1.081	34.56	1.0000
	2	1	1.053	-3.44	1.0000
		2	1.082	57.98	0.9999
		3	1.093	54.34	0.9999
	3	1	1.073	3.52	1.0000
		2	1.053	34.05	1.0000
		3	1.130	62.38	0.9999
	4	1	1.064	-51.46	1.0000
		2	1.051	36.20	0.9999
		3	1.024	-6.54	1.0000

Type	MSS No.	Calibration No.	slope	$intercept_Y$	R
CM1106	1	1	1.077	8.21	1.0000
		2	0.831	-320.26	0.9996
		3	1.061	-2.63	1.0000
	2	1	1.050	-20.05	1.0000
		2	1.030	-16.78	0.9999
		3	1.047	-13.41	0.9999
	3	1	1.064	27.16	1.0000
		2	1.041	31.71	1.0000
		3	1.103	53.97	1.0000
	4	1	1.086	-15.16	1.0000
		2	1.041	3.70	1.0000
		3	1.048	11.29	1.0000
MX1102	1	1	1.082	56.82	0.9999
		2	1.044	63.27	0.9998
		3	1.070	16.20	1.0000
	2	1	1.097	180.69	0.9998
		2	1.112	188.50	0.9994
		3	1.120	178.74	0.9997
	3	1	1.137	388.04	0.9983
		2	1.141	299.95	0.9994
		3	1.165	283.39	0.9996
	4	1	1.037	-43.99	1.0000
		2	0.994	-31.35	0.9998
		3	0.996	-49.51	0.9999

Table A2: data of MSS 1: mean factor f_m for each MOX-GS, its standard deviation $SD(f_m)$ [% f_m], maximum CO_2 concentration $c(CO_2)_{max}$ [vol.-ppm], percentage of measurement time with $c(CO_2)$ > 1000 vol.-ppm [POT] and conditions of measurement (DM = duration of measurement [h], NP = maximum number of persons in the room) room volume = 354 m³, maximum values, minimum values.

No.	Start of measurm.	DM [h]	NP max	c(CO_2) max [vol.-ppm]	POT	f_m						$SD(f_m)$					
						c(CO_2) > 1000 vol.-ppm			c(CO_2) ≤ 1000 vol.-ppm			c(CO_2) > 1000 vol.-ppm			c(CO_2) ≤ 1000 vol.-ppm		
						CCS	SGP	IDT 1	CCS	SGP	IDT 1	CCS	SGP	IDT 1	CCS	SGP	IDT 1
1	02.10. 14:00	48.8	2	588	0				9.172	1.093	1.295				43.3	11.1	28.7
2	04.10. 14:45	64.5	2	573	0				1.113	0.974	1.012				21.8	13.6	27.9
3	07.10. 07:15	24.4	3	728	0				8.726	1.053	1.003				57.1	17.3	27.1
4	08.10. 07:35	24.0	2	577	0				3.730	2.102	0.892				87.5	175.2	13.9
5	09.10. 07:11	23.5	2	540	0				1.920	1.369	1.106				33.2	7.5	25.2
6	10.10. 06:40	32.5	3	683	0				5.861	1.237	0.847				53.4	10.7	25.7
7	11.10. 15:09	65.0	4	737	0				1.371	1.416	1.277				33.1	12.8	23.2
8	14.10. 08:09	26.3	2	633	0				1.799	1.533	1.304				67.8	54.6	31.2
9	15.10. 10:28	24.4	2	635	0				2.280	1.348	1.208				53.5	17.3	30.4
10	16.10. 10:51	23.9	5	840	0				2.825	1.296	1.194				70.4	28.9	18.5
11	17.10. 10:42	28.0	2	690	0				2.286	1.358	1.172				94.3	24.0	31.5
12	18.10. 14:46	65.2	4	773	0				1.890	1.135	1.286				52.9	44.5	18.9
13	21.10. 08:00	24.5	2	641	0				4.185	1.038	0.994				40.1	32.2	16.4
14	22.10. 08:29	23.9	4	784	0				1.624	1.045	0.949				26.8	29.3	24.2
15	23.10. 08:23	24.0	2	630	0				1.607	1.151	0.944				32.7	27.9	13.5
16	24.10. 08:25	29.2	2	687	0				1.706	1.295	0.780				52.1	21.8	7.3
17	25.10. 14:06	66.2	2	557	0				2.704	1.181	0.916				53.9	17.3	18.0
18	28.10. 08:56	22.7	2	648	0				2.795	1.095	1.141				40.7	43.5	20.4
19	29.10. 07:36	6.7	2	638	0				5.450	1.018	0.720				86.7	17.7	4.6
20	30.10. 14:34	17.7	2	543	0				2.067	0.890	1.424				32.6	14.2	20.9
21	31.10. 08:16	31.0	2	552	0				1.750	1.220	1.105				37.2	13.6	23.0
22	01.11. 15:19	62.4	2	508	0				2.014	1.653	1.053				74.0	9.0	22.8
23	04.11. 05:46	26.0	2	556	0				2.258	1.701	0.837				38.0	9.3	5.7
24	05.11. 07:47	23.9	2	569	0				1.517	1.528	0.868				25.3	5.9	4.9
25	06.11. 07:44	24.4	2	569	0				2.949	1.591	0.886				85.0	10.9	12.0
26	07.11. 08:09	29.5	2	578	0				2.214	1.253	1.043				84.5	30.0	16.9
27	08.11. 14:29	65.6	2	546	0				2.813	1.159	1.105				55.5	19.9	17.0
28	11.11. 08:07	23.7	3	727	0					1.265	0.885					10.5	16.3
29	12.11. 07:50	23.9	2	537	0				1.182	1.764	1.086				19.9	14.0	18.8
30	13.11. 07:48	24.5	6	1198	0.05	1.202	1.404	0.495	2.174	1.771	0.969	10.1	32.1	7.0	92.3	31.2	12.8

No.	Start of measurm.	DM [h]	NP max	$c(CO_2)$ max [vol.-ppm]	POT	f_m						$SD(f_m)$					
						$c(CO_2) > 1000$ vol.-ppm			$c(CO_2) \leq 1000$ vol.-ppm			$c(CO_2) > 1000$ vol.-ppm			$c(CO_2) \leq 1000$ vol.-ppm		
						CCS	SGP	IDT 1	CCS	SGP	IDT 1	CCS	SGP	IDT 1	CCS	SGP	IDT 1
31	14.11. 08:20	26.6	5	1066	0.02	0.456	0.546	0.385	0.921	1.511	1.033	1.1	0.0	1.8	8.3	12.0	20.7
32	15.11. 14:10	66.1	2	513	0				1.786	1.208	1.239				29.4	23.1	15.1
33	18.11. 08:28	23.3	2	650	0				1.136	1.434	0.931				42.9	12.8	23.6
34	19.11. 07:49	48.4	2	669	0				1.983	1.414	0.976				65.8	9.7	19.5
35	21.11. 08:15	29.7	2	583	0				0.911	1.268	0.950				20.0	12.8	7.0
36	22.11. 14:28	65.9	2	523	0				1.406	1.137	1.223				26.5	28.7	14.0
37	25.11. 08:24	30.0	2	582	0				1.015	1.562	1.017				12.7	12.6	11.1
38	27.11. 14:39	17.6	2	536	0				0.925	1.371	0.930				6.0	10.2	6.4
39	28.11. 08:15	29.4	2	609	0				3.810	1.666	1.025				68.0	24.4	31.5
40	29.11. 14:04	66.2	2	542	0				2.337	1.131	0.999				41.7	17.3	18.5
41	02.12. 08:17	23.5	2	571	0				1.215	1.519	0.846				26.5	5.4	6.2
42	03.12. 07:56	23.8	2	543	0				3.510	1.612	0.978				74.4	22.7	25.5
43	04.12. 07:45	24.9	2	578	0				2.255	1.030	1.102				42.8	20.6	20.5
44	05.12. 08:42	29.6	2	689	0				0.976	1.237	0.960				17.3	6.3	19.6
45	06.12. 14:55	65.5	2	576	0				3.364	1.360	1.058				56.9	6.1	17.9
46	09.12. 08:28	23.4	2	612	0				8.510	1.466	0.849				50.7	6.4	6.0

Table A3: data of MSS 2: mean factor f_m for each MOX-GS, its standard deviation $SD(f_m)$ [% f_m], maximum CO_2 concentration $c(CO_2)_{max}$ [vol.-ppm], percentage of measurement time with $c(CO_2)$ > 1000 vol.-ppm [POT] and conditions of measurement (DM = duration of measurement [h], NP = maximum number of persons in the room) room volume = 52 m³, maximum values, minimum values.

No.	Start of measurm.	DM [h]	NP max	c(CO_2) max [vol.-ppm]	POT	f_m						$SD(f_m)$					
						c(CO_2) > 1000 vol.-ppm			c(CO_2) ≤ 1000 vol.-ppm			c(CO_2) > 1000 vol.-ppm			c(CO_2) ≤ 1000 vol.-ppm		
						CCS	SGP	IDT 1	CCS	SGP	IDT 1	CCS	SGP	IDT 1	CCS	SGP	IDT 1
1	01.10. 15:33	16.5	2	832	0				3.221	2.721	0.762				50.7	28.9	20.5
2	02.10. 08:04	54.8	3	1014	0.1	7.890	2.111	1.743	11.736	1.816	1.806	0.3	3.6	0.3	41.8	13.3	19.2
3	04.10. 14:55	65.4	2	605	0				10.160	1.658	2.543				61.2	7.3	13.7
4	07.10. 08:22	22.6	2	745	0				9.531	1.604	1.676				70.5	24.5	38.7
5	08.10. 06:58	24.3	3	1059	2.6	4.585	1.413	1.316	8.645	1.919	1.731	5.2	1.3	0.7	64.6	11.4	33.5
6	09.10. 07:16	24.8	2	946	0				0.686	2.147	1.122				9.0	10.5	7.9
7	10.10. 08:10	6.7	14/*	623	0				0.914	1.443	0.826				12.9	9.4	10.6
8	10.10. 15:42	25.2	4	1325	8.3	5.671	1.354	1.441	9.460	1.920	1.779	24.4	11.6	14.5	41.1	15.8	22.0
9	14.10. 08:09		2														
10	15.10. 07:06	23.9	2	1143	5.3	0.433	1.121	0.391	5.112	1.196	1.104	3.4	8.0	12.6	68.7	22.0	42.9
11	16.10. 07:02	9.8	3	1162	18.6	0.627	1.543	0.737	0.622	1.648	0.700	4.7	14.0	12.9	13.2	14.1	22.9
12	17.10. 10:42		2														
13	18.10. 14:12	65.8	2	608	0				5.912	2.036	2.404				81.6	83.8	79.4
14	21.10. 10:02	22.7	2	647	0				0.790	0.735	0.781				5.0	1.7	2.6
15	22.10. 08:45	23.6	2	627	0				0.737	0.699	0.788				2.9	1.9	7.2
16	23.10. 08:27	24.2	2	615	0				0.721	0.692	0.759				2.4	1.9	5.2
17	24.10. 08:41	28.9	2	662	0				0.721	0.964	0.861				2.7	16.5	9.9
18	25.10. 14:11	69.2	2	725	0				0.795	1.253	0.864				7.9	20.0	13.2
19	29.10. 14:05	24.8	3	1592	33.3	1.178	0.646	0.798	1.188	0.636	0.803	19.0	10.6	20.7	16.2	22.4	46.5
20	30.10. 14:59	17.2	2	1242	19.3	0.365	0.731	0.398	0.589	0.624	0.600	4.7	4.9	4.5	14.5	6.8	14.0
21	31.10. 08:23	30.5	2	938	0				0.782	0.888	0.797				12.5	15.9	6.9
22	01.11. 15:02	62.5	2	779	0				1.360	1.646	1.966				30.3	14.9	12.1
23	04.11. 14:57	16.9	2	938	0				1.519	1.786	1.759				21.2	8.7	9.1
24	05.11. 07:51	23.8	2	611	0				0.790	1.695	0.833				3.8	6.3	7.3
25	06.11. 09:38	22.5	2	871	0				0.866	1.245	1.551				24.6	16.1	27.3
26	07.11. 08:13	29.4	3	1551	35.5	0.476	0.901	0.526	0.625	0.972	0.626	14.3	7.9	20.0	32.6	12.6	22.7
27	08.11. 14:10	66.0	2	1171	2.1	0.585	0.960	0.794	0.958	1.103	0.824	15.2	3.1	2.4	10.7	12.4	10.5
28	11.11. 08:14	23.6	2	932	0				0.705	0.957	1.252				12.3	8.5	26.9
29	12.11. 07:54	23.9	2	1661	31.1	0.554	0.865	1.058	0.685	0.917	1.265	14.6	7.1	8.6	21.8	14.2	16.8
30	13.11. 07:54	24.2	5	2398	17.8	0.562	0.890	0.708	0.708	0.933	1.142	13.6	10.8	11.9	19.5	12.3	20.8

No.	Start of measurm.	DM [h]	NP max	$c(CO_2)$ max [vol.-ppm]	POT	f_m						$SD(f_m)$					
						$c(CO_2) > 1000$ vol.-ppm			$c(CO_2) \leq 1000$ vol.-ppm			$c(CO_2) > 1000$ vol.-ppm			$c(CO_2) \leq 1000$ vol.-ppm		
						CCS	SGP	IDT 1	CCS	SGP	IDT 1	CCS	SGP	IDT 1	CCS	SGP	IDT 1
31	14.11. 08:10	29.9	3	1556	25.7	0.694	1.100	0.731	0.614	0.918	0.666	18.5	26.3	24.2	13.5	18.8	22.0
32	15.11. 14:41	65.8	2	778	0				0.819	1.038	0.812				14.3	14.3	13.5
33	18.11. 08:38	23.3	2	1016	0.5	0.414	0.807	0.541	0.668	1.090	1.402	1.0	2.2	1.1	23.3	25.1	44.9
34	19.11. 09:08	47.1	2	1151	6.8	0.458	0.810	0.482	1.063	0.814	1.499	4.7	5.1	7.9	23.0	8.1	21.6
35	21.11. 08:24	29.6	2	533	0				0.917	1.222	0.975				5.9	9.9	9.4
36	22.11. 14:33	65.9	2	600	0				0.983	1.006	0.918				11.3	17.7	8.8
37	26.11. 14:59	17.6	2	990	0				0.651	1.442	1.237				13.2	5.2	7.9
38	27.11. 08:39	23.7	2	1195	19.1	0.488	1.580	0.681	0.576	1.499	0.587	14.8	22.9	20.3	11.2	6.6	12.3
39	28.11. 08:26	29.2	4	1416	27.6	0.378	1.039	0.676	0.605	1.335	1.308	10.9	9.6	43.0	14.2	10.1	18.0
40	29.11. 14:10	66.1	2	1090	0.5	0.384	0.897	0.597	0.820	1.042	0.825	3.2	2.9	2.2	13.7	8.7	12.8
41	02.12. 08:24	23.6	2	566	0				0.858	1.198	0.919				3.3	4.3	5.0
42	03.12. 08:03	23.7	2	609	0				0.854	1.349	0.956				6.8	9.9	9.6
43	04.12. 07:52	24.8	2	526	0				0.909	1.062	0.921				5.9	14.9	4.2
44	05.12. 08:48	29.5	2	530	0				0.902	1.089	1.002				3.4	7.1	5.4
45	06.12. 15:04	65.4	2	599	0				0.927	1.235	0.881				6.6	6.5	5.2

* room volume 130 m^3

Table A4: data of MSS 3: mean factor f_m for each MOX-GS, its standard deviation $SD(f_m)$ [% f_m], maximum CO_2 concentration $c(CO_2)_{max}$ [vol.-ppm], percentage of measurement time with $c(CO_2)$ > 1000 vol.-ppm [POT] and conditions of measurement (DM = duration of measurement [h], NP = maximum number of persons in the room) room volume = 44 m³, maximum values, minimum values.

No.	Start of measurm.	DM [h]	NP max	c(CO_2) max [vol.-ppm]	POT	f_m						$SD(f_m)$					
						c(CO_2) > 1000 vol.-ppm			c(CO_2) ≤ 1000 vol.-ppm			c(CO_2) > 1000 vol.-ppm			c(CO_2) ≤ 1000 vol.-ppm		
						CCS	SGP	IDT 1	CCS	SGP	IDT 1	CCS	SGP	IDT 1	CCS	SGP	IDT 1
1	03.10. 17:17	15.4	1	764	0				1.981	1.935	0.849				27.7	2.9	5.6
2	04.10. 14:51	64.8	2	1183	1.5		1.189	0.397		1.917	0.883		3.4	4.7		8.3	8.3
3	07.10. 07:34	23.6	3	1734	25.7	0.621	1.048	0.997	1.411	1.382	1.134	28.6	17.8	10.8	26.8	10.5	5.0
4	08.10. 07:10	23.9	4	1691	6.4	3.679	2.043	1.115	3.833	1.598	0.908	12.2	15.4	14.2	28.3	12.0	30.2
5	09.10. 07:05	23.3	2	673	0				5.548	1.786	2.081				19.4	8.2	7.7
6	10.10. 06:20	32.9	1	1221	10.8	6.534	1.299	1.487	4.861	1.592	0.891	11.7	35.2	13.8	33.8	17.8	58.8
7	11.10. 15:12	65.0	1	1005	0.2	0.524	1.119	0.593	0.722	1.686	0.733	1.0	0.7	0.5	24.1	13.6	14.5
8	14.10. 08:24	26.2	1	905	0				1.095	1.588	0.724				49.5	42.2	23.3
9	15.10. 10:33	24.3	1	915	0				2.529	1.325	1.623				79.3	14.0	42.0
10	16.10. 10:54	23.9	1	873	0				1.338	1.649	0.939				129.5	11.8	59.6
11	17.10. 10:47	27.7	2	1788	13.1	5.719	5.400	2.168	1.773	2.342	1.213	17.0	23.3	10.9	153.0	57.3	59.2
12	18.10. 14:35	65.8	1	1336	2.2	0.507	7.232	0.394	0.677	4.216	0.664	3.0	7.9	10.9	13.6	60.5	13.3
13	21.10. 08:25	24.2	2	1656	14.7	0.570	0.666	0.572	5.368	1.012	1.596	13.5	5.5	17.7	52.7	18.0	29.6
14	22.10. 08:38	24.0	2	1089	1.2	0.653	1.028	0.815	0.895	1.042	0.890	1.7	4.1	1.2	37.5	13.9	16.6
15	23.10. 08:36	23.9	2	1876	64.7	0.515	0.797	0.558	0.620	0.883	0.599	11.0	7.5	4.9	9.7	13.1	4.7
16	24.10. 08:35	28.9	1	1352	12.3	0.529	0.605	0.613	3.148	0.972	1.498	4.8	9.7	8.5	45.1	15.7	18.4
17	25.10. 14:25	69.2	1	1367	0.9	0.849	0.640	0.844	0.709	1.189	0.739	6.6	3.6	6.9	13.6	15.3	19.4
18	28.10. 11:49	19.9	2	1325	20.5	1.712	0.845	1.110	2.877	0.953	1.771	53.0	18.6	41.3	32.4	12.6	20.7
19	29.10. 07:46	30.2	2	2004	25.7	1.127	0.602	0.813	1.990	0.856	1.319	14.3	22.0	25.5	37.5	18.4	19.9
20	30.10. 14:34																
21	31.10. 17:54	16.1	2	507	0				0.878	0.856	0.879				3.7	2.0	1.8
22	01.11. 10:02	5.5	1	1087	33.8	5.972	1.150	0.620	6.179	1.295	0.684	3.3	2.9	3.0	18.4	5.7	3.8
23	01.11. 15:40	61.7	1	798	0				1.234	1.857	0.865				22.9	7.9	9.3
24	04.11. 05:25	26.6	2	1518	6	0.727	1.330	0.714	0.843	1.632	1.039	10.2	18.8	7.1	16.4	12.6	20.2
25	05.11. 08:05	24.2	2	2054	48.2	0.907	1.068	0.729	1.021	1.385	0.945	14.0	10.9	10.4	15.8	13.3	25.2
26	06.11. 08:02	23.9	2	1400	15.9	0.746	1.031	0.648	1.001	1.564	0.940	9.5	10.0	13.5	16.4	8.3	11.6
27	07.11. 15:07	29.5	2	1709	14.1	4.409	1.268	1.045	5.065	1.573	1.389	31.0	16.9	14.4	44.4	44.8	23.0
28	08.11. 08:18	65.4	2	1056	0.6	0.396	1.174	0.441	0.981	1.487	0.817	1.6	4.6	9.0	16.0	7.7	13.1
29	11.11. 08:30	23.6	2	1981	42.1	0.574	0.835	0.533	0.891	1.046	0.650	16.3	12.0	7.9	16.6	9.9	28.1
30	12.11. 08:08	23.9	1	2064	59.9	0.735	0.885	0.681	0.847	1.041	0.832	10.6	11.2	11.6	14.6	9.8	10.5

No.	Start of measurm.	DM [h]	NP max	c(CO_2) max [vol.-ppm]	POT	f_m						$SD(f_m)$					
						c(CO_2) > 1000 vol.-ppm			c(CO_2) ≤ 1000 vol.-ppm			c(CO_2) > 1000 vol.-ppm			c(CO_2) ≤ 1000 vol.-ppm		
						CCS	SGP	IDT 1	CCS	SGP	IDT 1	CCS	SGP	IDT 1	CCS	SGP	IDT 1
31	13.11. 08:03	24.4	1	1405	37.3	0.831	1.005	0.789	0.882	1.098	0.844	5.0	6.2	4.7	14.5	7.4	9.3
32	14.11. 08:32	29.8	2	1692	7.2	0.581	0.912	0.652	0.735	1.074	0.812	6.9	7.0	6.9	20.6	11.8	16.7
33	15.11. 14:18	66.6	1	814	0				1.134	1.098	0.830				23.9	8.1	8.6
34	18.11. 09:45	22.3	1	1227	9.9	0.447	0.843	0.552	0.640	1.070	0.658	6.1	7.0	3.9	13.2	11.2	13.4
35	19.11. 08:09	48.3	2	1854	23.9	2.065	0.776	1.063	2.980	1.009	1.675	15.7	6.8	11.4	28.0	10.3	17.5
36	21.11. 08:26	29.7	1	1324	18.3	0.559	0.776	0.641	0.806	1.103	0.930	10.7	13.8	14.1	14.6	15.9	15.8
37	22.11. 14:39	65.9	1	1284	4.2	0.369	0.954	0.491	0.768	1.175	0.767	6.1	13.1	7.0	11.5	27.3	14.0
38	25.11. 08:33	23.8	1	1091	3.5	1.273	0.633	0.796	1.586	1.095	0.981	4.0	32.9	2.6	25.9	32.8	12.7
39	26.11. 08:25	23.9	2	1730	19.3	1.300	0.761	0.817	1.590	1.022	1.207	12.3	12.3	12.3	20.0	15.3	14.2
40	27.11. 08:25	6.0	1	923	0				0.829	0.738	0.840				22.2	15.4	17.1
41	28.11. 15:56	21.8	1	1064	1.2	2.635	1.012	0.974	1.930	1.201	1.254	8.3	1.8	3.3	47.1	11.5	22.8
42	29.11. 14:17	66.2	1	1342	3.8	0.341	0.896	0.430	0.795	1.226	0.828	5.7	8.9	6.4	11.7	3.1	9.4
43	02.12. 08:29	23.9	1	631	0				1.151	1.020	0.927				17.7	7.3	6.4
44	03.12. 08:24	23.6	1	646	0				0.802	1.115	0.857				6.7	9.4	8.1
45	04.12. 08:01	25.8	1	780	0				0.668	0.994	0.796				6.2	15.2	9.9
46	05.12. 09:47	28.6	2	1593	39.4	1.089	0.773	0.570	0.957	0.803	0.570	32.0	9.1	17.3	44.0	15.1	23.6
47	06.12. 15:11	65.4	1	1472	5.3	0.384	1.263	0.440	0.724	1.236	0.731	27.7	91.9	6.9	14.4	12.3	22.2

Table A5: data of MSS 4: mean factor f_m for each MOX-GS, its standard deviation $SD(f_m)$ [% f_m], maximum CO_2 concentration $c(CO_2)_{max}$ [vol.-ppm], percentage of measurement time with $c(CO_2)$ > 1000 vol.-ppm [POT] and conditions of measurement (DM = duration of measurement [h], NP = maximum number of persons in the room) room volume = see footnotes, maximum values, minimum values.

No.	Start of measurm.	DM [h]	NP max	c(CO_2) max [vol.-ppm]	POT	f_m						$SD(f_m)$					
						c(CO_2) > 1000 vol.-ppm			c(CO_2) ≤ 1000 vol.-ppm			c(CO_2) > 1000 vol.-ppm			c(CO_2) ≤ 1000 vol.-ppm		
						CCS	SGP	IDT 1	CCS	SGP	IDT 1	CCS	SGP	IDT 1	CCS	SGP	IDT 1
1	04.10. 14:43	64.4	1/a	507	0				1.034	3.070	3.193				19.4	5.6	18.4
2	07.10. 07:34	23.6	*														
3	08.10. 07:23	4.0	9/b	1930	21.9	1.249	2.506	0.765	0.967	1.908	0.785	8.6	23.7	9.8	17.0	25.6	17.4
4	09.10. 06:58	23.6	6/b	1333	3.5	0.673	1.256	0.649	0.817	2.173	0.842	4.2	5.6	3.5	8.3	11.1	7.7
5	11.10. 06:46	3.6	3/b	829	0				0.836	2.285	0.849				9.7	5.1	8.7
6	11.10. 15:06	65.0	2/a	779	0				0.875	2.134	0.858				12.1	9.3	10.5
7	14.10. 10:58	5.8	10/c	2138	36.1	0.558	1.467	0.551	0.694	1.606	0.696	17.0	9.8	21.6	13.3	18.4	12.1
8	14.10. 16:53	42.1	7/b	1751	7.9	1.676	1.419	0.638	0.920	1.694	0.894	51.9	16.3	38.3	31.4	13.8	20.1
9	16.10. 11:05	21.5	28/d	1964	14.9	0.539	2.040	0.726	0.712	1.965	0.782	8.4	7.7	8.6	15.7	6.9	24.8
10	17.10. 08:41	23.4	7/c	2935	24.5	1.936	1.326	0.853	2.856	1.738	1.309	17.1	11.1	26.6	21.7	12.5	17.2
11	18.10. 08:16	5.9	7/e	1398	0.3	0.373	0.905	0.554	0.761	2.215	1.107	10.9	8.5	10.2	22.6	47.6	43.3
12	18.10. 14:25	65.8	1/b	664	0				0.881	2.111	1.144				8.1	37.6	19.5
13	21.10. 08:14	24.3	7/b	1897	19.3	0.752	1.191	0.794	0.737	1.451	0.840	29.6	18.6	15.0	7.6	12.0	12.0
14	22.10. 08:34	1.5	9/b	1592	58.3	0.493	0.943	0.676	0.650	1.251	0.718	4.5	7.7	4.3	9.9	4.8	6.0
15	23.10. 08:33	23.9	6/b	1402	4.5	0.612	0.363	0.692	1.624	0.873	1.589	12.6	6.7	5.2	28.9	18.2	22.7
16	24.10. 08:30	23.9	8/b	1542	3.7	0.566	0.660	0.707	1.570	1.038	1.255	7.4	10.7	6.2	30.8	12.7	20.3
17	25.10. 08:30	4.8	8/c	1313	43.7	0.485	0.825	0.665	0.637	1.213	0.827	5.1	4.4	6.8	8.2	10.7	7.2
18	25.10. 14:20	69.2	7/b	1511	1.4	0.696	0.778	0.787	0.962	1.235	1.170	4.3	8.3	7.0	7.5	16.4	17.1
19	28.10. 11:46	20.5	4/b	1176	1	1.334	1.120	1.123	1.503	0.978	1.906	5.5	4.5	6.0	17.7	11.8	19.1
20	29.10. 07:36	25.5	9/b	2188	5.1	1.126	2.099	0.866	2.385	1.017	1.778	37.5	40.2	14.9	36.8	21.8	33.3
21	30.10. 14:42	17.8	1/b	639	0				0.858	1.115	1.078				6.2	16.8	12.9
22	31.10. 08:27	9.0	1/b	529	0				1.015	1.128	1.101				7.8	10.1	13.7
23	01.11. 15:26	62.1	1/d	570	0				1.568	1.572	1.336				28.9	18.2	18.9
24	04.11. 05:30	9.1	30/d	1788	37.6	0.789	1.232	0.838	0.910	1.726	0.957	5.3	6.0	7.0	5.5	10.9	4.7
25	04.11. 14:40	17.3	1/b	677	0				0.848	1.961	0.891				10.3	5.3	9.4
26	05.11. 08:01	23.9	8/b	1651	7.2	0.790	1.221	1.156	1.000	1.807	1.923	18.6	36.8	16.2	12.1	9.7	22.2
27	06.11. 07:56	24.4	8/b	1664	1.7	0.539	1.122	0.745	1.483	1.851	2.267	10.1	13.0	8.9	42.2	10.4	36.4
28	07.11. 08:28	29.2	4/c	1880	16.6	1.145	1.362	1.129	1.647	1.594	1.657	15.4	34.2	13.2	27.0	22.0	20.5
29	11.11. 08:25	23.6	6/b	1411	7.6	1.268	1.106	0.775	1.081	1.585	1.290	11.1	19.8	14.3	12.6	12.2	24.1
30	12.11. 08:05	23.9	8/b	1669	12.9	1.582	1.232	0.572	1.200	1.792	1.517	10.4	15.4	38.2	24.4	9.9	29.5

No.	Start of measurm.	DM [h]	NP max	$c(CO_2)$ max [vol.-ppm]	POT	f_m						$SD(f_m)$					
						$c(CO_2)$ > 1000 vol.-ppm			$c(CO_2) \leq$ 1000 vol.-ppm			$c(CO_2)$ > 1000 vol.-ppm			$c(CO_2) \leq$ 1000 vol.-ppm		
						CCS	SGP	IDT 1	CCS	SGP	IDT 1	CCS	SGP	IDT 1	CCS	SGP	IDT 1
31	13.11. 08:00	22.9	8/b	1921	21.8	1.953	1.649	0.573	0.971	1.742	1.034	35.5	22.5	39.7	29.3	6.5	14.6
32	14.11. 07:02	31.3	6/c	2224	13.1	0.543	1.322	0.782	0.987	1.749	1.751	12.4	10.7	13.5	22.2	13.7	28.2
33	15.11. 14:27	66.3	1/c	605	0				1.542	1.941	2.157				20.3	9.8	11.1
34	18.11. 08:51	23.4	10/c	3617	10	0.448	1.407	0.670	1.249	1.715	1.510	17.0	15.2	7.9	27.9	12.7	22.3
35	19.11. 08:16	48.4	1/c	2377	5.6	0.442	1.955	0.798	1.050	1.646	1.207	7.8	17.4	18.9	22.9	9.6	24.2
36	21.11. 08:39	29.4	1/c	698	0				0.845	1.456	0.989				14.0	16.3	18.4
37	22.11. 14:37	65.8	1/c														
38	25.11. 08:30		*														
39	26.11. 08:20	23.9	9/b	1871	12.4	1.462	1.285	0.700	1.248	1.522	0.933	8.7	18.0	18.3	16.7	8.8	17.0
40	27.11. 08:13	24.3	9/b	1870	9.9	0.928	1.174	0.774	0.986	1.694	1.074	29.5	10.1	11.2	11.1	9.7	11.4
41	28.11. 08:35	5.9	9/b	1726	21.2	0.713	1.151	0.768	0.865	1.567	0.829	8.2	11.7	7.4	24.3	12.5	12.7
42	29.11. 15:05	65.3	1/b	542	0				2.744	1.101	1.299				24.9	13.1	15.0
43	02.12. 08:15	24.0	*														
44	03.12. 08:00	24.0	*														
45	04.12. 08:00	24.9	5/b	1506	2.5	1.145	0.875	0.372	2.493	1.309	0.808	8.3	11.4	32.7	26.0	82.0	16.2
46	05.12. 08:49	25.0	7/b	1601	6.7	2.242	0.892	0.700	1.045	1.354	1.656	88.8	15.8	22.9	16.7	9.9	18.6
47	06.12. 15:06	65.7	1/b	1776	2.6	1.854	0.911	0.528	1.016	1.663	1.089	6.9	12.1	29.5	12.3	6.0	14.9
48	09.12. 12:00	20.6	12/c	3549	72	0.368	1.122	0.569	0.523	1.299	0.676	14.4	22.9	13.0	6.8	11.3	6.0

Footnote	a	b	c	d	e	*
room volume [m^3]/ information	354	51	90	339	158	sensor dropout

Selected measurements with clusters of maxima or minima are highlighted at the next page in Fig. A1 and A2 to provide further information on possible reasons why the algorithms tend to larger deviations between $e(CO_2)$ and $c(CO_2)_m$ values. It seems that the gradients and absolute concentrations during the first minutes after start of measurement play an important role for the precision of correlation of both values. This hypothesis could be proved with more details if the mathematical schemes of the algorithms are considered. If the hypothesis is true, several large deviations between $e(CO_2)$ and $c(CO_2)_m$ values found in this campaign with daily new start of the sensors, will not occur during long-term applications of the algorithms, since the sensors will operate then continuously without daily new start. The arrows in Fig. A1 and A2 indicate the relevant y-axis for each curve.

Fig. A1: Courses of $e(CO_2)$ and $c(CO_2)_m$ values during the measurements No. 2 (left) and No. 20 (right) of MSS 2, arrows indicate the relevant y-axis

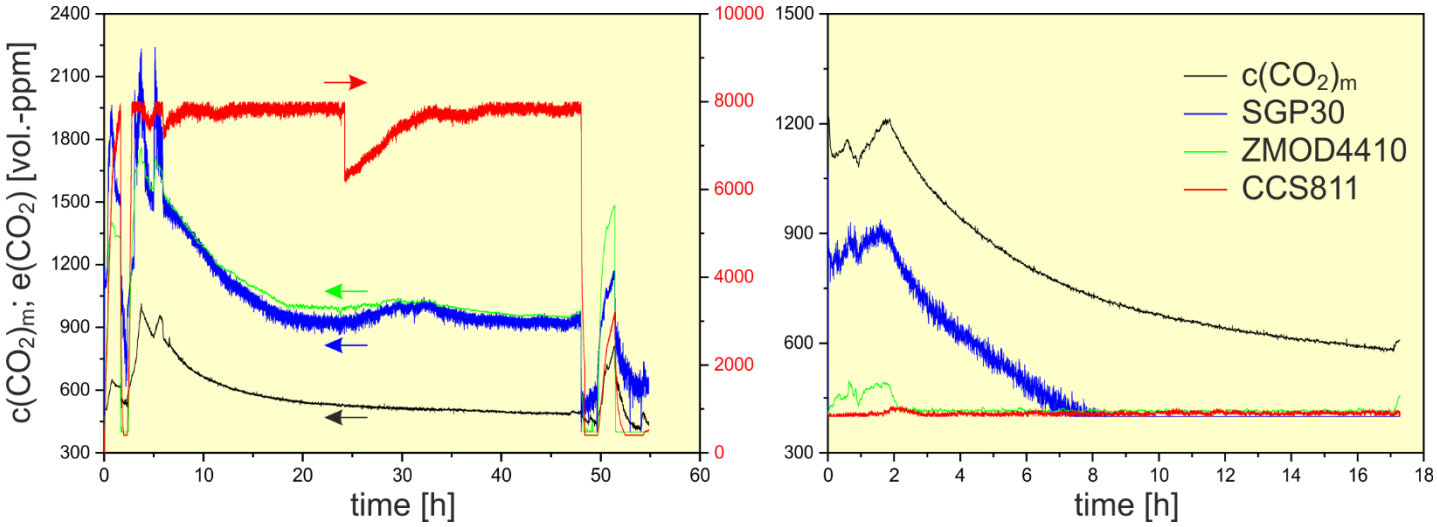

Fig. A2: Courses of $e(CO_2)$ and $c(CO_2)_m$ values during the measurem. No. 12 of MSS 3 (left) and No. 48 of MSS 4 (right), arrows indicate the relevant y-axis.